



## RESEARCH LETTER

10.1002/2014GL061715

## Key Points:

- Oscillating brittle-ductile deformation processes explained by energy feedback
- Multiscale time-space observations in the Glarus thrust explained by one model
- The Glarus thrust exposes spatial patterns of episodic fluid-release slip events

## Correspondence to:

T. Poulet,  
Thomas.poulet@csiro.au

## Citation:

Poulet, T., M. Veveakis, M. Herwegh, T. Buckingham, and K. Regenauer-Lieb (2014), Modeling episodic fluid-release events in the ductile carbonates of the Glarus thrust, *Geophys. Res. Lett.*, *41*, 7121–7128, doi:10.1002/2014GL061715.

Received 29 AUG 2014

Accepted 9 OCT 2014

Accepted article online 11 OCT 2014

Published online 29 OCT 2014

## Modeling episodic fluid-release events in the ductile carbonates of the Glarus thrust

Thomas Poulet<sup>1</sup>, Manolis Veveakis<sup>1</sup>, Marco Herwegh<sup>2</sup>, Thomas Buckingham<sup>2</sup>, and Klaus Regenauer-Lieb<sup>3</sup>

<sup>1</sup>CSIRO Mineral Resources, Bentley, Western Australia, Australia, <sup>2</sup>Institute of Geological Sciences, University of Bern, Bern, Switzerland, <sup>3</sup>School of Petroleum Engineering, University of New South Wales, Sydney, New South Wales, Australia

**Abstract** The exposed Glarus thrust displays midcrustal deformation with tens of kilometers of displacement on an ultrathin layer, the principal slip zone (PSZ). Geological observations indicate that this structure resulted from repeated stick-slip events in the presence of highly overpressured fluids. Here we show that the major characteristics of the Glarus thrust movement (localization, periodicity, and evidence of pressurized fluids) can be reconciled by the coupling of two processes, namely, shear heating and fluid release by carbonate decomposition. During this coupling, slow ductile creep deformation raises the temperature through shear heating and ultimately activates the chemical decomposition of carbonates. The subsequent release of highly overpressurized fluids forms and lubricates the PSZ, allowing a ductile fault to move tens of kilometers on millimeter-thick bands in episodic stick-slip events. This model identifies carbonate decomposition as a key process for motion on the Glarus thrust and explains the source of overpressured fluids accessing the PSZ.

### 1. Introduction

Due to its spectacular and unique appearance as a sharp line in the landscape (Figure 1a), the Glarus thrust in the Swiss Alps has fascinated scientists for more than 150 years as recognized by the United Nations Educational, Scientific and Cultural Organization [UNESCO, 2014]. In the mid-1800s, Escher von der Linth first suggested the idea of a single thrust, which finally became accepted at the beginning of the twentieth century [Heim, 1922]. By the late 1960s to 1980s, it was evident that the movement of thick nappes on a thin thrust plane was difficult to explain by the traditional concepts of mechanics. Hence, the concepts of thrust lubrication were developed to overcome this paradox [Hsü, 1969; Hubbert and Rubey, 1959; Schmid *et al.*, 1977]. The experimental study of Schmid *et al.* [1977] demonstrated that such localized lubrication effects may be due to prolonged ductile deformation. Subsequent geochemical studies have identified slip-correlated chemical alterations [Herwegh *et al.*, 2008b; Hürzeler and Abart, 2008] and postulated the presence of pressurized fluids causing hydrofractures on the thrust plane [Badertscher and Burkhard, 2000; Badertscher *et al.*, 2002; Burkhard *et al.*, 1992; Ebert *et al.*, 2007a; Ring *et al.*, 2001].

Recently, a theory for episodic slip events was presented based on fluid-release reactions triggered by ductile creep [Alevizos *et al.*, 2014]. The theory was applied to subduction megathrust for the case of serpentinite dehydration and reproduced the temporal evolution recorded by GPS and seismic signals [Alevizos *et al.*, 2014; Poulet *et al.*, 2014; Veveakis *et al.*, 2014]. We propose here that the same theory applied to a different mineralogy can be used to understand the key aspects of the spatial observations in the Glarus thrust. In the following, we present an overview of the relevant geological observations followed by a concise summary of the model and a discussion of its possible application.

### 2. Field Observations

The Glarus thrust is characterized in Figure 1b by multiple localization features in space and time. The pervasively deformed zone at the core of the thrust is termed the “fault core” [Sibson, 2003] and is less than a meter thick at the most localized northern thrust, increasing toward the southern, deeper end of the thrust to several meters thickness. Outside of the fault core, both in the hanging wall and footwall, chemical-mechanical deformation is much less intense, and in some places, the rock even appears intact [Ebert *et al.*, 2007a].

Within the mechanically deformed fault core, two markedly different regimes can be identified in the field. A central knife-sharp principal slip zone (PSZ) (Figures 1b and 1c) [Sibson, 2003], also known as the septum

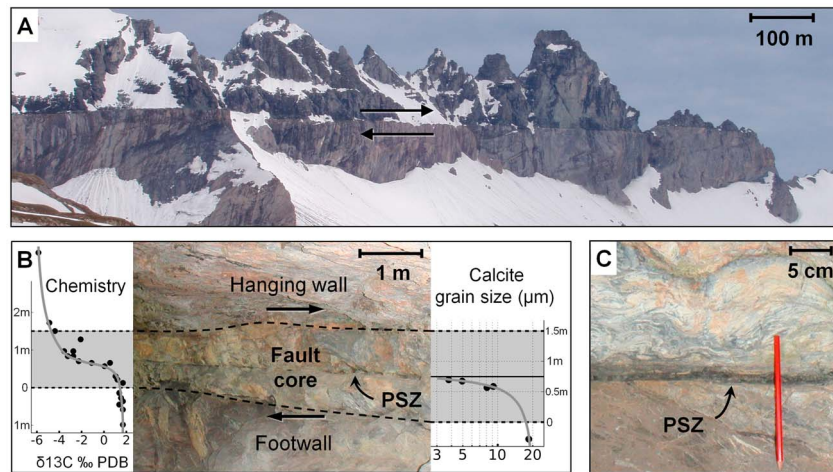


**Figure 1.** Photos from the Glarus thrust (Alps) illustrating the spatial cascade of deformation on three different scales: (a) The Nappe has moved on a very sharp boundary at the kilometer scale (Lochsiten location, see *Herwegh et al.* [2008b]). (b) A closer look reveals a meter-wide fault core, at the (c) center of which an ultralocalized centimeter-thick most recent PSZ is clearly visible. The left inset of Figure 1b shows a steep gradient of stable carbon isotopes [*Herwegh et al.*, 2008b]), transitioning from the hanging wall chemistry to the footwall. This chemical gradient is accompanied by mechanical deformation, as evidenced by the formation of the PSZ and the sharp reduction of the average calcite grain size [*Ebert et al.*, 2007a; *Herwegh et al.*, 2008b]) in the fault core (right inset of Figure 1b).

[see *Ebert et al.*, 2007a, and references therein], is surrounded by the Lochsiten calc-mylonite, which exhibits intense ductile deformation, as well as brittle events of fracturing and calcite veining. It also provides clear evidence of chemical alteration and mixing of the footwall and hanging wall, expressed for example through the gradient of the carbon isotopes (Figure 1b).

In the fault core, ductile dynamic recrystallization [*Ebert et al.*, 2007a] is recorded through progressive reduction in calcite grain size toward the PSZ (Figure 1b). The PSZ itself does not follow the ductile deformation pattern of the fault core but displays distinct deformation events under brittle conditions as evidenced by hydraulic fractures shown in Figure 2a (inset).

The simple planar appearance of the Glarus thrust belies a complex and long-lasting time evolution [*Ebert et al.*, 2007a; *Herwegh et al.*, 2008b; *Pfiffner*, 1980]. Microstructural and geothermometric investigations [*Ebert et al.*, 2007a] reveal multiple brittle events interrupting ductile deformation along the thrust, as evidenced by recurrently folded calcite veins (Figure 2a). This sequence is illustrated by ultrafine-grained (<2  $\mu\text{m}$ ) mylonites in the northern exposures of the thrust, changing to somewhat coarser-grained mylonites (3–20  $\mu\text{m}$ ) for the hotter conditions in the south, the latter being dominated by dislocation creep as the major deformation mechanism.

The superposition of brittle and ductile deformation structures in space and time is therefore cascading over three spatial scales (Nappe: kilometer scale, fault core: meter scale, and PSZ: millimeter scale) and two time scales (slow ductile creep and fast slip on the PSZ). To date, there is no plausible explanation for juxtaposition and reciprocal overprinting of brittle and ductile deformation styles at these elevated metamorphic conditions. Access of an overpressured fluid to the thrust could explain the switch from slow ductile to fast brittle deformation. However, we argue that the mechanism delivering overpressured fluids remains undetermined and the episodic nature remains unexplained.

This is one of the reasons for the long-lasting debate on the origins and associated deformation mechanisms of the Glarus thrust. However, this thrust is not unique as similar episodic slip events are inferred all along the Helvetic Alps at similar crustal levels [*Badertscher and Burkhard*, 2000; *Herwegh et al.*, 2008a] as well as in other thrusts around the world [*Kennedy and Logan*, 1997; *Molli et al.*, 2011].

We suggest that the problem can be resolved by considering the overall displacement of the Nappe (~40 km) as a stick-slip phenomenon in the ductile realm, with seismically active episodic fast slip events followed by ductile aseismic creep. In the following, we will test a model that is capable of reconciling the spatial and

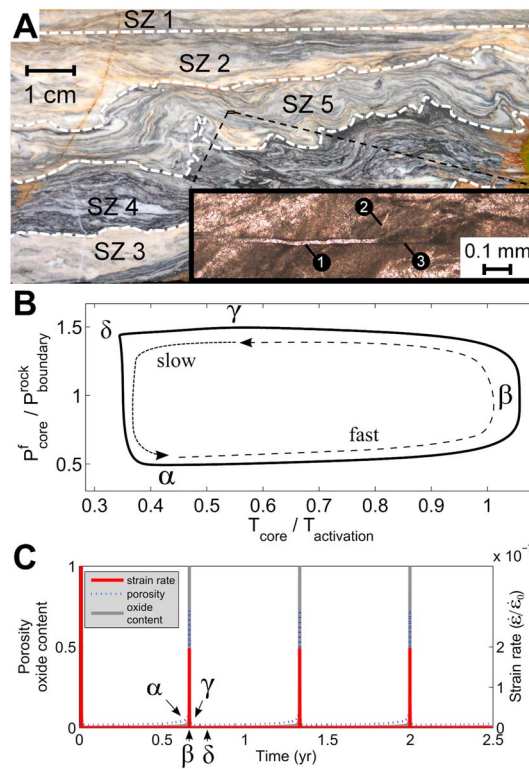


**Figure 2.** (a) Episodic brittle-ductile behavior of the Glarus thrust is clearly demonstrated through multiple subparallel slip zones (SZn). Each white band (CaCO<sub>3</sub>) corresponds to a single former vein calcite layer evolved in the PSZ. The arrays of SZs are accumulated and folded, indicating passive deformation of the older SZs, while ambient deformation was accommodated in a new planar slip zone (see inset). The different arrays of old slip zones are folded (SZ2–SZ5) and overprinted by ductile deformation, while the youngest slip zones still show their planar geometry. The inset shows an example of a hydrofracture on one PSZ. The (1) hydrofracture branches into a (2) diagonal offshoot with the (3) shear plane continuing along the slip direction. This calcite mineralization setting is akin to a pseudotachylyte injection feature in granitic systems, where the melting-recrystallization process is replaced here by carbonate decomposition/precipitation. The difference resides in the activation energy of the two reactions, with carbonate decomposition (300–650°C)/precipitation being admitted at much lower temperatures than melting (on the order of 1200°C)/recrystallization. (b) Phase diagram in  $p_f$ - $T$  space showing the cyclic behavior at the center of the PSZ as described in text. (c) Cyclic time evolution of the modeled oscillator. The strain rate ( $\dot{\epsilon}$ ), porosity (equal to the volume ratio of produced CO<sub>2</sub>), and volumetric content of oxide (CaO) highlight the stick-slip nature of the process. The parameter values used are listed in Table 1.

standard power law ductile rheology. The key ingredient of the physics considered in this model is mechanical dissipation appearing as viscous shear heating [Duretz et al., 2014] that produces the heat required to trigger carbonate decomposition (see discussion on chemical reactions capping the uncontrolled temperature rise from shear heating in Veveakis et al. [2010]), which in turn will release supercritical CO<sub>2</sub> causing chemical pressurization, i.e., the buildup of a CO<sub>2</sub> pore fluid pressure. The corresponding system of equation reduces to a couple set of reaction diffusion equations for temperature  $T$  and excess pore fluid pressure  $p_f$  [Alevizos et al., 2014].

temporal complexities. This model is based on first principles and can explain the episodic release of overpressured fluids by in situ fluid-release reactions.

### 3. The Model

Laboratory experiments [Han et al., 2007], theoretical studies [Sulem and Famin, 2009], and geological observations of mineralogy and chemical alteration patterns [Collettini et al., 2013; Famin et al., 2008; Herwegh et al., 2008b] independently suggest that carbonate decomposition and precipitation are the key reactions during seismic events. Based on the carbonate-rich nature of the Glarus rocks, we adopt this suggestion as the reaction controlling the primary alteration in the fault core. Carbonate decomposition ( $\pm$ water) is an endothermic reaction and so requires the addition of heat to be activated. The generated CO<sub>2</sub> behaves as a supercritical fluid at depth, and the oxides, being highly unstable, could also react further with other minerals or water if present. Knowing for the importance of these water-associated reactions in the natural cases, we neglect them for the moment for the purpose of highlighting the principal processes only and discuss the process on the example of the water absent chemical reaction. We therefore consider a generic formulation for solid breakdown reaction of the type  $AB_{\text{solid}} \xrightarrow[\omega_R]{\omega_F} A_{\text{solid}} + B_{\text{fluid}}$  and apply the theory from equation (6) in Poulet et al. [2014] to carbonates, with all equations and corresponding parameters defined therein.

Microstructural observation on the deformation mechanism place the Glarus thrust (location Lochsite) in conditions of ductile creep, at about 7–8 km depth, having an ambient temperature  $T_b$  of around 220°C and a lithostatic pressure of around 200 MPa [e.g., Ebert et al., 2007a]. Within the framework for episodic tremor and slip events [Poulet et al., 2014], we use plate tectonic boundary conditions to drive the movement of the hanging wall and footwall. Based on geological and experimental observations, we apply in the fault core a

The system is characterized by three main dimensionless groups: (i) the Gruntfest number  $Gr$  defined as the ratio of the energy input through mechanical work divided by the energy (enthalpy) required for the reaction, (ii) the modified Lewis number  $\bar{L}e$  expressing the ratio of chemical over hydraulic diffusivities [Poulet *et al.*, 2014], and (iii) the ratio  $K_c$  of the preexponential factors of the kinetics of the forward over the reverse reaction. Asymptotic and numerical analyses for this system of equations reveal three fundamental steady state regimes, determined by the eigenvalues of the solutions [Alevizos *et al.*, 2014; Veveakis *et al.*, 2014]. Depending on the values of the parameters and initial conditions, the fault can creep in a stable manner or assume instabilities that are either solitary or periodic. Based on the field evidence (Figure 2a), we are interested in the periodic regime, which is admitted when the following inequalities are met simultaneously [Alevizos *et al.*, 2014; Poulet *et al.*, 2014; Veveakis *et al.*, 2014]

$$Gr > \left(1 + \frac{e^{Ar \theta_b}}{Ar \delta}\right) e^{-\alpha Ar}, \quad \bar{L}e < Ar^{-3/2}, \quad \log(K_c) \gg 1 \quad (1)$$

where  $Ar = Q_F/(RT_C)$  and  $\alpha = 1 - Q_d/Q_F$ . In these expressions,  $Q_F$  is the activation enthalpy of the forward chemical reaction,  $Q_d$  is the activation enthalpy of the rheology, and  $Ar$  is the Arrhenius number expressing the extent of the reaction with activation enthalpy  $Q_F$  taking place at reference temperature  $T_C$ . The quantity  $\theta_b = (T_b - T_C)/T_C$  is the dimensionless boundary temperature, and  $\delta \ll 1$  is the ratio of the energy sinks of the problem, i.e., the enthalpy of the endothermic reaction divided by the thermal conductivity of the system [see Alevizos *et al.*, 2014]. As this formulation is generic, it can be applied to multiple chemical reactions using the principle of linear superposition [Law, 2006]. The transient regimes can be resolved numerically [Veveakis *et al.*, 2014] and can reveal chaotic system behavior that can be applied to specific case studies [Poulet *et al.*, 2014].

Here we use this model to test the validity of the assumption that carbonate decomposition could be a key driver of the Glarus thrust evolution. We assume that the system is chemically closed and isolated from external fluids. This means that there is no net loss or gain of volume or mass through the boundaries of the mechanically deformed fault core and the conservation of the chemical species is ensured. Therefore, any fluids have to either be preexistent and in equilibrium with their host or generated from solid phase breakdown. Note that this simplification is in contrast to the observations of the Glarus thrust, where an open system with infiltration and exfiltration of fluids has been suggested in various studies [e.g., Badertscher *et al.*, 2002; Hürzeler and Abart, 2008]. As stated above, however, we keep the system as simple as possible for the moment in order to unravel the effect of first-order processes.

The periodic regime is characterized by a multiphysics oscillator in the fluid pressure ( $p_f$ )-temperature ( $T$ ) phase diagram (Figure 2b). Starting at any  $p_f$  and  $T$ , the evolution of the  $p_f$  and  $T$  conditions will converge on a stable limit cycle. For example, from the creeping flow regime, temperature slowly increases ( $\delta$  to  $\alpha$ ) due to shear-heating-outpacing thermal diffusion. When temperature exceeds point  $\alpha$ , the cycle evolves rapidly (Figure 2c). The temperature increases abruptly up to the activation of the reaction, while the pore pressure increases slightly due to the fluid compressibility. The reaction then releases supercritical  $\text{CO}_2$ , increasing fluid pressure and porosity until a maximum value of porosity and strain rate (point  $\beta$ ). Past this point, temperature decreases while fluid pressure becomes sufficiently high to cause hydraulic fractures (point  $\gamma$ ). The fluid now lubricates the depleted central part of the shear zone, and the diffusion slowly brings the system from point  $\gamma$  to point  $\delta$ , from which it slowly creeps back to point  $\alpha$ . Since full reversibility of the chemical reaction was assumed, this cycle will then repeat itself indefinitely (Figure 2b). Note that in the present approach, the fracture process itself is not implemented.

#### 4. Results

The puzzling spatial observations of three length scales (Nappe, fault core, and PSZ) are tested by our model, and we present its overall calibration process for all the dimensionless parameters listed in Poulet *et al.* [2014]. We start by recalling from Poulet *et al.* [2014] that the two length scales of the fault core thickness ( $h$ , on the order of 1 m) and PSZ ( $d$ , on the order of 1 mm) are correlated, respectively, to the Zel'dovich numbers of the rheology and (forward) chemical reactions

$$d \sim \mathcal{O}\left(\frac{RT_b^2}{Q_d}\right), \quad h \sim \mathcal{O}\left(\frac{RT_b^2}{Q_F}\right) \quad (2)$$

**Table 1.** Input Parameters Used for Numerical Simulation<sup>a</sup>

Symbol	Name	Unit of Measure	Value	Literature Values
$T_b$	Boundary temperature	°C	220	220–230 [Herwegh et al., 2008b]
$\Delta P_b$	Boundary excess fluid pressure	MPa	0	-
$\phi_0$	Reference porosity	-	0.01	-
$\rho_{CaCO_3}$	Calcium carbonate density	kg/m <sup>3</sup>	2710	2710 [Sulem and Famin, 2009]
$\rho_{CaO}$	CaO density	kg/m <sup>3</sup>	3350	3350 [Sulem and Famin, 2009]
$\rho_{CO_2}$	Carbon dioxide density	kg/m <sup>3</sup>	900	800–1200 [Sulem and Famin, 2009]
$M_{CaCO_3}$	Calcium carbonate molar mass	kg/mol	0.1	0.1 [Sulem and Famin, 2009]
$M_{CaO}$	CaO molar mass	kg/mol	0.056	0.056 [Sulem and Famin, 2009]
$M_{CO_2}$	Carbon dioxide molar mass	kg/mol	0.044	0.044 [Sulem and Famin, 2009]
$C$	Heat capacity	J/(kg C)	1000	1000 [Sulem and Famin, 2009]
$c_{th}$	Thermal diffusivity	m <sup>2</sup> /s	10 <sup>-6</sup>	10 <sup>-6</sup> [Alevizos et al., 2014]
$K_c$	Equilibrium constant	-	7.10 <sup>8</sup>	10 <sup>2</sup> –10 <sup>20</sup> [L'Vov, 2007]
$m$	Material rate sensitivity	-	3	3–9 [Herwegh et al., 2003]
$\dot{\epsilon}_0$	Reference strain rate	1/s	10 <sup>8</sup>	10 <sup>5</sup> –10 <sup>11</sup> [Brodie and Rutter, 2000]
$\Lambda$	Pressurization coefficient	MPa/°C	10 <sup>-3</sup>	10 <sup>-4</sup> –1 [Cecinato 2011; Rice 2006]
$\beta_f + \beta_s$	Compressibility	Pa <sup>-1</sup>	10 <sup>-7</sup>	10 <sup>-9</sup> –1.4 × 10 <sup>-5</sup> [Sulem and Famin, 2009; Zhang and Reeder, 1999]
$\mu_f$	Fluid viscosity	Pa s	10 <sup>-4</sup>	10 <sup>-4</sup> [Sulem and Famin, 2009]
$d$	Fault core thickness	m	1.5	0.5–5 (field observation)
$k_f$	Forward preexponential factor	s <sup>-1</sup>	7.10 <sup>9</sup>	1E2–1E69 [L'Vov et al., 2002]
$k_r$	Reverse preexponential factor	s <sup>-1</sup>	10	-
$\Delta h$	Specific enthalpy of the reaction	kJ/mol	100	47–3800 [L'Vov et al., 2002]
$Q_F$	Activation enthalpy of forward reaction	kJ/mol	207	47–3800 [L'Vov et al., 2002]
$Q_R$	Activation enthalpy of reverse reaction	kJ/mol	103	-
$k_0$	Reference permeability	m <sup>2</sup>	5 × 10 <sup>-18</sup>	-
$Q_d$	Activation enthalpy of the rheology	kJ/mol	103	190–426 kJ/mol [Brodie and Rutter, 2000; Herwegh et al., 2003]
$\sigma_n$	Normal overstress	MPa	0.1	-
$\tau_n$	Shear overstress	MPa	0.2	-

<sup>a</sup>Refer to Alevizos et al. [2014] for the definition of the model parameters and more detailed explanation of the theory.

The 2 orders of magnitude difference observed,  $h \sim 10^2 d$  (Figure 1b), imply that  $Q_F \approx 2Q_d$ , and therefore,  $\alpha = 0.5$ .

The geological and mineralogical conditions considered (carbonate-rich thrust at 7 km depth) match the example presented in Table 1 and Appendix A of Alevizos et al. [2014], and we can therefore use the parameter values presented there. In particular, we set  $Ar = 40$ ,  $\delta = 2.6 \times 10^{-3}$ , and  $\theta_b = -0.2$  and calibrate the remaining dimensionless parameters against the spatial and temporal field observations reported in the previous section. The value of  $Q_F \approx 210$  kJ/mol is then determined from the values of  $Ar$ ,  $\theta_b$ , and  $T_b$ . Since  $\alpha = 0.5$ , this value  $Q_F$  would provide an activation energy for the rheology  $Q_d \approx 105$  kJ/mol, that is smaller than for the case of pure calcite (see Table 1). This result would imply a polymineralic nature of the fault core's matrix.

Alternating structures consisting of greyish host rock and white calcite veins transformed by subsequent ductile deformation into mylonites (Figure 2a) suggest episodic brittle-ductile events in the Glarus thrust within the fault core. Although there is no quantitative timing of the slip events, these observations constrain the system to be in its periodic regime and therefore to obey equation (1). From these inequalities,  $Gr$  and  $\bar{L}e$  can therefore be selected close to their critical values,  $Gr = 10^{-5}$  and  $\bar{L}e = 70$ .

The spatial observations of the exposed thrust allow for a more quantitative calibration of the model. The widths of the observed PSZ and chemical alteration zone (Figure 3a) can be explained by the interplay of mechanics and chemistry as shown in Figure 3b and allow us to set the values of the remaining groups by matching the numerical results (Figure 3b) with the field observations (Figure 3a). Veveakis et al. [2014] showed that the spatial extent of the chemical mixing zone (area 2 in Figure 3a) depends either on  $K_c$  or on the normalized enthalpy of the reaction  $x = \Delta H/Q_F$ , where  $\Delta H = Q_F - Q_R$  is the enthalpy of the reaction defined as the difference of the forward and reverse values. The two are equivalent, and we fix therefore  $x = 0.5$  [Alevizos et al., 2014] and invert the value  $K_c = 7 \times 10^8$ . Based on the retrieved values of all dimensionless groups, we invert for a given set of the underlying physical parameters (Table 1). All inverted values are in

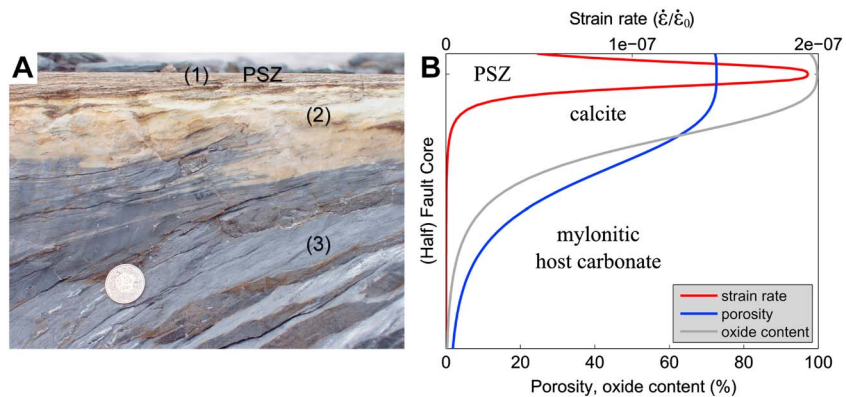


**Figure 3.** (a) Details of the fault core of the Glarus thrust (Vorab location) [Herwegh *et al.*, 2008b]. (1) A mixture of carbonate and Verrucano defines the youngest PSZ. Below the PSZ a complex zone of (2) yellowish-white calcite veins fingering into the (3) mylonitic greyish host carbonate of the fault core is visible. The complex zone shows the signs of both chemical and mechanical mixing. Image modified from Herwegh *et al.* [2008b]. (b) Numerically generated results showing the profiles of the strain rate  $\dot{\epsilon}$ , porosity (chemically produced  $\text{CO}_2$ ), and volumetric content of oxide (CaO) across the fault core on the most recent slip event (point  $\beta$  in Figure 2b). The co-location of mechanical deformations and chemical alterations is as observed in Figure 3a, highlighting the causal relationship between those two phenomena. The mechanism also suggests that fluid originates from the PSZ, producing  $\text{CO}_2$  at maximum fluid pressures exceeding lithostatic stress (Figure 2b) and injecting the produced fluids into the mylonitic host carbonate as seen in Figure 2a. The reverse reaction precipitates significant portions of calcite in a distinct zone surrounding the PSZ.

the ranges reported in the literature for calcite decomposition/precipitation, pointing it as the dominant carbonate driving this oscillator.

The resulting slip instability is marked by a rapid increase in strain rate that is tightly localized into a central PSZ, where the carbonate has been decomposed (Figure 2c). The strain rate on the central PSZ increases by at least 5 orders of magnitude during the instability (Figure 2c), reproducing the observed dichotomy (stick slip, Figure 2a) in deformation styles. Starting with an initial value of 1 vol %, the porosity in the PSZ reaches 70 vol % along a narrow slip plane in a short period of instability in which the carbonate is depleted. The temperature increase depends on both the percentage of carbonate that reacts and the activation temperature of the breakdown reaction and the preexistence of a hydrous phase. The absolute value of the maximum temperature reached is determined by the activation temperature of the decomposition reaction selected. In this paper we have considered carbonate decomposition as the driving reaction, without specifying its exact nature. Field evidence at the Spoleto thrust [Collettini *et al.*, 2013] suggests  $\text{CaCO}_3$  decomposition/precipitation as the dominant reaction, in which case the activation temperature would be in excess of to  $650^\circ\text{C}$  [Rodríguez-Navarro *et al.*, 2009]. However, the presence of  $\text{MgCO}_3$  could reduce the activation temperature as low as  $330^\circ\text{C}$  [LVov, 2007] or even lower in the presence of hydrates. To date, no field evidence has been documented of such decomposition for the Glarus; yet the coexistence of calcite and dolomite in the Glarus tectonites pleads in favor of such reduced decomposition temperatures. In any case, we emphasize that the chemical cycle is a confined (Figure 3b) and short-lived event as the temperature only remains above  $300^\circ\text{C}$  for less than 36 h in the most extreme case of  $\text{CaCO}_3$  in  $\text{CO}_2$  (Figure 2c). Circumstantial evidence of such heat can be inferred from the resetting of the microstructure from earlier slip through thermal overprint of the latest event. We observe indeed a grain size profile with a single minimum around the latest PSZ (Figure 1b) instead of the expected various local minima corresponding to all PSZs (Figure 2a). Stable phases that record such tectonothermal events and conclusively determine the nature of the chemical reaction are expected to be of nanometer scale, and investigations at that scale using novel techniques [Savage *et al.*, 2014] should be encouraged. Note that the thermal reset can occur within hours for the fault core conditions considered here [Covey-Crump, 1997], making a proof of the existence of decomposition products very difficult after the long exhumation history after the seismic initiation.

## 5. Discussion and Conclusion

We have approached the Glarus thrust field observations by a first-order, multiphysics analysis which investigates the fundamental material behavior. The puzzling spatiotemporal sequence can be explained by

a carbonate oscillator, which self consistently switches from slow to fast modes under a critical driving force without any arbitrary external influence (such as imposed stick-slip boundary conditions or highly pressurized fluid input). In our model, the Nappe is seen to creep on a fault core, which through its ductile creep process raises slowly the temperature by shear heating. At a critical moment when the heat triggers the endothermic carbonate breakdown reaction, the system switches to a fast, ultralocalized slip event on the central PSZ. When the carbonate on the PSZ is almost entirely consumed, the fast slip stops, and the exothermic reaction of oxides with CO<sub>2</sub> forms new carbonates. After the breakdown, the system cools within hours down to the ambient temperature conditions of the host rock. Although we have considered a carbonate breakdown reaction, the same type of instability will occur under more complicated and perhaps more realistic mineralogical transitions involving the release of a hydrous fluid phase. There is certainly much uncertainty for the laboratory-determined parameters; however, dimensionless groups provide the ability to absorb such uncertainties.

In nature, the temporal evolution of the shear zone is likely to become more complex. For example, the highly reactive solid oxides (like CaO or MgO) may seek alternative reactions (e.g., forming hydroxides in the presence of water), or fluids may infiltrate and escape [Badertscher *et al.*, 2002; Hürzeler and Abart, 2008]. Also, the predicted fluid pressures on the PSZ are so high that hydraulic fractures (not modeled here but observed in the case of the Glarus thrust; see Figure 2 and Badertscher and Burkhard [2000] and Ebert *et al.* [2007a]) must be a consequence of the oscillator. Furthermore, secondary metamorphic reactions can be triggered under far from equilibrium conditions. In addition, along the 40 km of the thrust, the behavior may change from the grain-size insensitive dislocation creep to diffusion creep [Ebert *et al.*, 2007b]. These alterations would imply different spatiotemporal evolutions. Since the purpose of this work is to expose the fundamental chemomechanical oscillator for the Glarus thrust, such effects have not been included in the present work and would need further research in the future.

Based on the outcomes of this study, a long-lasting debate on the need of the carbonate as lubricants of the Glarus thrust may be solved [see Herwegh *et al.*, 2008b] as it is a critical component to activate the aforementioned process. We postulate that this signature deformation sequence of carbonate rocks in the ductile regime is universal and rationalizes the origin of fluids in compressive ductile environments [Miller, 2013]. We suggest that because of its fundamental character, this mechanism may be observed in many geological outcrops, where shear heating causes chemical decomposition reactions. Similar examples to the Glarus thrust can indeed be found in the field. The McConnell thrust in the Rocky Mountains [Kennedy and Logan, 1997] and the Naukluft thrust in Namibia [Rowe *et al.*, 2012] both feature a fault core and a central PSZ. We postulate that many more such systems can be found also involving other signature oscillators with different decomposition or dewatering reactions such as clay minerals, chlorite, mica, dolomite, calcite, and serpentinite involved in ductile shear zones.

#### Acknowledgments

The manuscript is self contained and can be reproduced by the person skilled in the art with the help of the references provided in the paper. The formulation itself is published in Alevizos *et al.* [2014], Poulet *et al.* [2014], and Veveakis *et al.* [2014]. The data used consist of the numerical values presented in Table 1 and the equation from the above cited articles; the geological material provided is accessible in the referenced literature.

The Editor thanks two anonymous reviewers for their assistance in evaluating this paper.

#### References

- Alevizos, S., T. Poulet, and E. Veveakis (2014), Thermo-poro-mechanics of chemically active creeping faults. 1: Theory and steady state considerations, *J. Geophys. Res. Solid Earth*, *119*, 4558–4582, doi:10.1002/2013JB010070.
- Badertscher, N. P., and M. Burkhard (2000), Brittle-ductile deformation in the Glarus thrust Lochseiten (LK) calc-mylonite, *Terra Nova*, *12*(6), 281–288.
- Badertscher, N. P., R. Abart, M. Burkhard, and A. McCaig (2002), Fluid flow pathways along the Glarus overthrust derived from stable and Sr-isotope patterns, *Am. J. Sci.*, *302*(6), 517–547.
- Brodie, K. H., and E. H. Rutter (2000), Deformation mechanisms and rheology: Why marble is weaker than quartzite, *J. Geol. Soc.*, *157*(6), 1093–1096.
- Burkhard, M., R. Kerrich, R. Maas, and W. S. Fyfe (1992), Stable and Sr-isotope evidence for fluid advection during thrusting of the Glarus nappe (Swiss Alps), *Contrib. Mineral. Petrol.*, *112*(2–3), 293–311.
- Cecinato, F., A. Zervos, and E. Veveakis (2011), A thermo-mechanical model for the catastrophic collapse of large landslides, *Int. J. Numer. Anal. Methods Geomech.*, *35*, 1507–1535, doi:10.1002/nag.963.
- Collettini, C., C. Viti, T. Tesei, and S. Mollo (2013), Thermal decomposition along natural carbonate faults during earthquakes, *Geology*, *41*, 927–930.
- Covey-Crump, S. J. (1997), The normal grain growth behaviour of nominally pure calcitic aggregates, *Contrib. Mineral. Petrol.*, *129*(2–3), 239–254.
- Duretz, T., S. M. Schmalholz, Y. Y. Podladchikov, and D. A. Yuen (2014), Physics-controlled thickness of shear zones caused by viscous heating: Implications for crustal shear localization, *Geophys. Res. Lett.*, *41*, 4904–4911, doi:10.1002/2014GL060438.
- Ebert, A., M. Herwegh, and A. Pfiffner (2007a), Cooling induced strain localization in carbonate mylonites within a large-scale shear zone (Glarus thrust, Switzerland), *J. Struct. Geol.*, *29*(7), 1164–1184.
- Ebert, A., M. Herwegh, B. Evans, A. Pfiffner, N. Austin, and T. Vennemann (2007b), Microfabrics in carbonate mylonites along a large-scale shear zone (Helvetic Alps), *Tectonophysics*, *444*(1–4), 1–26.
- Famin, V., S. Nakashima, A.-M. Boullier, K. Fujimoto, and T. Hirono (2008), Earthquakes produce carbon dioxide in crustal faults, *Earth Planet. Sci. Lett.*, *265*(3–4), 487–497.

- Han, R., T. Shimamoto, T. Hirose, J.-H. Ree, and J.-I. Ando (2007), Ultralow friction of carbonate faults caused by thermal decomposition, *Science*, 316(5826), 878–881.
- Heim, A. (1922), *Geologie der Schweiz. 2: Die Schweizer Alpen*, Tauchnitz, Leipzig, Germany.
- Herwegh, M., X. Xiao, and B. Evans (2003), The effect of dissolved magnesium on diffusion creep in calcite, *Earth Planet. Sci. Lett.*, 212(3), 457–470.
- Herwegh, M., A. Berger, A. Ebert, and S. Brodhag (2008a), Discrimination of annealed and dynamic fabrics: Consequences for strain localization and deformation episodes of large-scale shear zones, *Earth Planet. Sci. Lett.*, 276(1–2), 52–61.
- Herwegh, M., J.-P. Hürzeler, O. A. Pfiffner, S. Schmid, R. Abart, and A. Ebert (2008b), The Glarus thrust: Excursion guide and report of a field trip of the Swiss Tectonic Studies Group (Swiss Geological Society, 14–16. 09. 2006), *Swiss J. Geosci.*, 101(2), 323–340.
- Hsü, K. J. (1969), A preliminary analysis of the statics and kinetics of the Glarus overthrust, *Eclogae Geol. Helv.*, 62, 143–154.
- Hubbert, K. M., and W. W. Rubey (1959), Role of fluid pressure in mechanics of overthrust faulting: I. Mechanics of fluid-filled porous solids and its application to overthrust faulting, *Geol. Soc. Am. Bull.*, 70(2), 115–166.
- Hürzeler, J.-P., and R. Abart (2008), Fluid flow and rock alteration along the Glarus thrust, *Swiss J. Geosci.*, 101(2), 251–268.
- Kennedy, L. A., and J. M. Logan (1997), The role of veining and dissolution in the evolution of fine-grained mylonites: The McConnell thrust, Alberta, *J. Struct. Geol.*, 19(6), 785–797.
- Law, C. K. (2006), *Combustion Physics*, pp. 738–738, Cambridge Univ. Press, Cambridge, U. K.
- L'Vov, B. V. (2007), *Thermal Decomposition of Solids and Melts*, 246 pp., Springer, New York.
- L'Vov, B. V., L. K. Polzik, and V. L. Ugolkov (2002), Decomposition kinetics of calcite: A new approach to the old problem, *Thermochim. Acta*, 390(1), 5–19.
- Miller, S. A. (2013), Chapter 1 - The role of fluids in tectonic and earthquake processes, in *Advances in Geophysics*, edited by R. Dmowska, pp. 1–46, Elsevier, Amsterdam, Netherlands.
- Molli, G., J. C. White, L. Kennedy, and V. Taini (2011), Low-temperature deformation of limestone, Isola Palmaria, northern Apennine, Italy - The role of primary textures, precursory veins and intracrystalline deformation in localization, *J. Struct. Geol.*, 33(3), 255–270.
- Pfiffner, O. A. (1980), Strain analysis in folds (Infrahelvetic complex, Central Alps), *Tectonophysics*, 61(4), 337–362.
- Poulet, T., E. Veveakis, K. Regenauer-Lieb, and D. A. Yuen (2014), Thermo-poro-mechanics of chemically active creeping faults: 3. The role of serpentinite in episodic tremor and slip sequences, and transition to chaos, *J. Geophys. Res. Solid Earth*, 119, 4606–4625, doi:10.1002/2014JB011004.
- Rice, J. R. (2006), Heating and weakening of faults during earthquake slip, *J. Geophys. Res.*, 111, B05311, doi:10.1029/2005JB004006.
- Ring, U., M. T. Brandon, and A. Ramthun (2001), Solution-mass-transfer deformation adjacent to the Glarus Thrust, with implications for the tectonic evolution of the Alpine wedge in eastern Switzerland, *J. Struct. Geol.*, 23(10), 1491–1505.
- Rodriguez-Navarro, C., E. Ruiz-Agudo, A. Luque, A. B. Rodriguez-Navarro, and M. Ortega-Huertas (2009), Thermal decomposition of calcite: Mechanisms of formation and textural evolution of CaO nanocrystals, *Am. Mineral.*, 94(4), 578–593.
- Rowe, C. D., A. Fagereng, J. A. Miller, and B. Mapani (2012), Signature of coseismic decarbonation in dolomitic fault rocks of the Naukluft Thrust, Namibia, *Earth Planet. Sci. Lett.*, 333 – 334, 200–210.
- Savage, H. M., P. J. Polissar, R. Sheppard, C. D. Rowe, and E. E. Brodsky (2014), Biomarkers heat up during earthquakes: New evidence of seismic slip in the rock record, *Geology*, 42(2), 99–102.
- Schmid, S. M., J. N. Boland, and M. S. Paterson (1977), Superplastic flow in finegrained limestone, *Tectonophysics*, 43(3–4), 257–291.
- Sibson, R. H. (2003), Thickness of the Seismic Slip Zone, *Bull. Seismol. Soc. Am.*, 93(3), 1169–1178.
- Sulem, J., and V. Famin (2009), Thermal decomposition of carbonates in fault zones: Slip-weakening and temperature-limiting effects, *J. Geophys. Res.*, 114, B03309, doi:10.1029/2008JB006004.
- UNESCO (2014), World Heritage Swiss Tectonic Arena Sardona. [Available at <http://www.unesco-sardona.ch>]
- Veveakis, E., S. Alevizos, and I. Vardoulakis (2010), Chemical reaction capping of thermal instabilities during shear of frictional faults, *J. Mech. Phys. Solids*, 58(9), 1175–1194.
- Veveakis, E., T. Poulet, and S. Alevizos (2014), Thermo-poro-mechanics of chemically active creeping faults: 2. Transient considerations, *J. Geophys. Res. Solid Earth*, 119, 4583–4605, doi:10.1002/2013JB010071.
- Zhang, J., and R. J. Reeder (1999), Comparative compressibilities of calcite-structure carbonates; deviations from empirical relations, *Am. Mineral.*, 84(5–6), 861–870.